Coupling of Metal-Based Light-Harvesting Antennas and Electron-Donor Subunits: Trinuclear Ruthenium(II) Complexes Containing Tetrathiafulvalene-Substituted Polypyridine Ligands

Sebastiano Campagna,*[a] Scolastica Serroni,[a] Fausto Puntoriero,[a] Frédérique Loiseau,[a] Luisa De Cola,*[b] Cornelis J. Kleverlaan,[b] Jan Becher,*[c] Ane Ploug Sørensen,[c] Philippe Hascoat,[d] and Niels Thorup[e]

Abstract: Three new tetrathiafulvalene-substituted 2,2′-bipyridine ligands, *cis*-bpy-TTF_1, *trans*-bpy-TTF_1, and *cis*-bpy-TTF_2 have been prepared and characterized. X-ray analysis of *trans*-bpy-TTF_1 is also reported. Such ligands have been used to prepare two new trinuclear Ru^{II} complexes, namely, $[\{(bpy)_2Ru(\mu\text{-}2,3\text{-}dpp)\}_2Ru(bpy\text{-}TTF_1)](PF_6)_6$ (**9**; bpy = 2,2′-bipyridine; 2,3-dpp = 2,3-bis(2′-pyridyl)pyrazine) and $[\{(bpy)_2Ru(\mu\text{-}2,3\text{-}dpp)\}_2Ru(bpy\text{-}TTF_2)](PF_6)_6$ (**10**). These compounds can be viewed as coupled antennas and charge-separation systems, in which the multichromophoric trinuclear metal subunits act as light-harvesting antennas and the tetrathiafulvalene electron donors can induce charge separation. The absorption spectra, redox behavior, and luminescence properties (both at room temperature in acetonitrile and at 77 K in a rigid matrix of butyronitrile) of the trinuclear metal complexes have been studied. For the sake of completeness, the mononuclear compounds $[(bpy)_2Ru(bpy\text{-}TTF_1)](PF_6)_2$ (**7**) and $[(bpy)_2Ru(bpy\text{-}TTF_2)](PF_6)_2$ (**8**) were also synthesized and studied. The properties of the tetrathiafulvalene-containing species were compared to those of the model compounds $[Ru(bpy)_2(4,4'\text{-}Mebpy)]^{2+}$ (4,4′-Mebpy = 4,4′-dimethyl-2,2′-bipyridine) and $[\{(bpy)_2Ru(\mu\text{-}2,3\text{-}dpp)\}_2Ru(bpy)]^{6+}$. The absorption spectra and redox behavior of all the new metal compounds can be interpreted by a multicomponent approach, in which specific absorption features and redox processes can be assigned to specific subunits of the structures. The luminescence properties of the complexes in rigid matrices at 77 K are very similar to those of the corresponding model compounds without TTF moieties, whereas the new species are nonluminescent, or exhibit very weak emissions relative to those of the model compounds in fluid solution at room temperature. Time-resolved transient absorption spectroscopy confirmed that the potentially luminescent MLCT states of **7**–**10** are significantly shorter lived than the corresponding states of the model species. Photoinduced electron-transfer processes from the TTF moieties to the (excited) MLCT chromophore(s) are held responsible for the quenching processes.

Keywords: electron transfer · ligand design · photochemistry · ruthenium · time-resolved spectroscopy

[a] Prof. Dr. S. Campagna, Prof. Dr. S. Serroni, Dr. F. Puntoriero, Dr. F. Loiseau
Dipartimento di Chimica Inorganica Chimica Analitica e Chimica Fisica
Università di Messina, 98166 Messina (Italy)
E-mail: photochem@chem.unime.it

[b] Prof. Dr. L. De Cola, Dr. C. J. Kleverlaan
Institute of Molecular Chemistry, Molecular Photonics Group
Universiteit van Amsterdam, 1018 WV Amsterdam (The Netherlands)
E-mail: ldc@science.uva.nl

[c] Prof. Dr. J. Becher, Dr. A. P. Sørensen
Department of Chemistry, SDU
University of Southern Denmark, 5230 Odense M (Denmark)
E-mail: jbe@chem.sdu.dk

[d] Dr. P. Hascoat
UMR CNRS 6510 Synthèse et Electrosynthèse Organique
Université de Rennes I (France)

[e] Prof. Dr. N. Thorup
Department of Chemistry, Technical University of Denmark
2800, Lyngby (Denmark)
E-mail: nt@kemi.dtu.dk

Introduction

The design of artificial systems that can act as antennas and charge-separation species—the two basic systems operating in the primary processes of photosynthesis—is an important research field, mainly because the development of efficient artificial systems for photochemical energy conversion would have a major impact on society.[1] This has stimulated much research, and interesting artificial antenna[2] and charge-separation[3] systems have been reported over the last two decades. However, multicomponent species containing both antenna and charge-separation subunits are extremely rare.[4] Intuitively, the most convenient way to interface antenna and charge separation subunits is direct coupling of the energy trap (i.e., the site of the antenna to which the light energy collected by all the chromophores is channeled) and an electron-donor/acceptor subunit.

  0947-6539/02/0819-4461 $ 20.00+.50/0

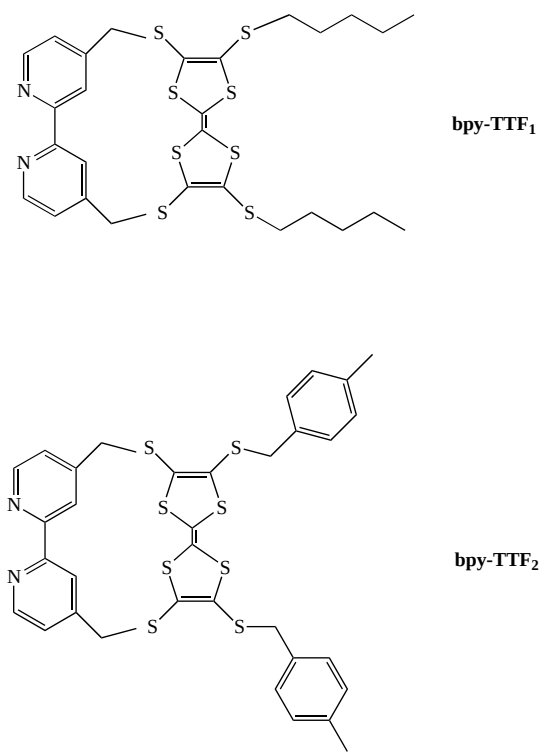

Scheme 1. Structural formulas of bpy-TTF_1 and bpy-TTF_2.

As a first step towards the coupling of antenna and charge-separation subunits, we report the synthesis, luminescence, and redox properties of two new ruthenium complexes containing multichromophoric subunits that act as solar-energy absorbers and electron-donor subunits that induce charge separation. As the multichromophore subunit, we used a trinuclear ruthenium(II) species which is itself a multi-component compound and has been employed as a component of metal-based dendrimers that function as light-harvesting antennas.[5] As the electron-donor subunit, we used two tetrathiafulvalene (TTF) moieties covalently linked to 2,2′-bipyridine (bpy). The TTF electron donors were selected due to their stability and favorable redox properties.[6] The trinuclear compounds investigated were $[\{(bpy)_2Ru(\mu\text{-}2,3\text{-}dpp)\}_2Ru(bpy\text{-}TTF_1)](PF_6)_6$ (**9**; 2,3-dpp = 2,3-bis(2′-pyridyl)-pyrazine) and $[\{(bpy)_2Ru(\mu\text{-}2,3\text{-}dpp)\}_2Ru(bpy\text{-}TTF_2)](PF_6)_6$ (**10**). Scheme 1 shows structural formulas of the ligands. For reference, the mononuclear compounds $[(bpy)_2Ru(bpy\text{-}TTF_1)](PF_6)_2$ (**7**) and $[(bpy)_2Ru(bpy\text{-}TTF_2)](PF_6)_2$ (**8**) have also been synthesized and studied. Preparation of the bpy-TTF_1 and bpy-TTF_2 ligands (Scheme 2) followed the effective dealkylation/alkylation protocol developed in one of our laboratories.[7] The ligand bpy-TTF_1 was obtained as a mixture of *trans* and *cis* isomers. However, *trans*-bpy-TTF_1 isomerizes to the *cis* isomer under the reaction conditions used to prepare the metal complexes, and identical final products were obtained from both isomers. Hence, in complexes, bpy-TTF_1 denotes exclusively the *cis* isomer.

Results and Discussion

The structure of *trans*-bpy-TTF_1 was determined by X-ray crystallography (Figure 1). The long axis of the TTF part is staggered with respect to the long axis of the bipyridine component of the ligand. The two *trans*-oriented chains are both extended, but in different directions. One chain is slightly inclined toward the TTF part, whereas the other chain is considerably inclined toward the TTF part and extended towards the bipyridine moiety.

Cyclic and differential pulse voltammetry experiments indicated that the new compounds **7**–**10** all undergo multiple reversible oxidation and reduction processes in acetonitrile within the potential window investigated (+1.8 to −1.0 V versus SCE; Table 1). Each process was assigned to specific

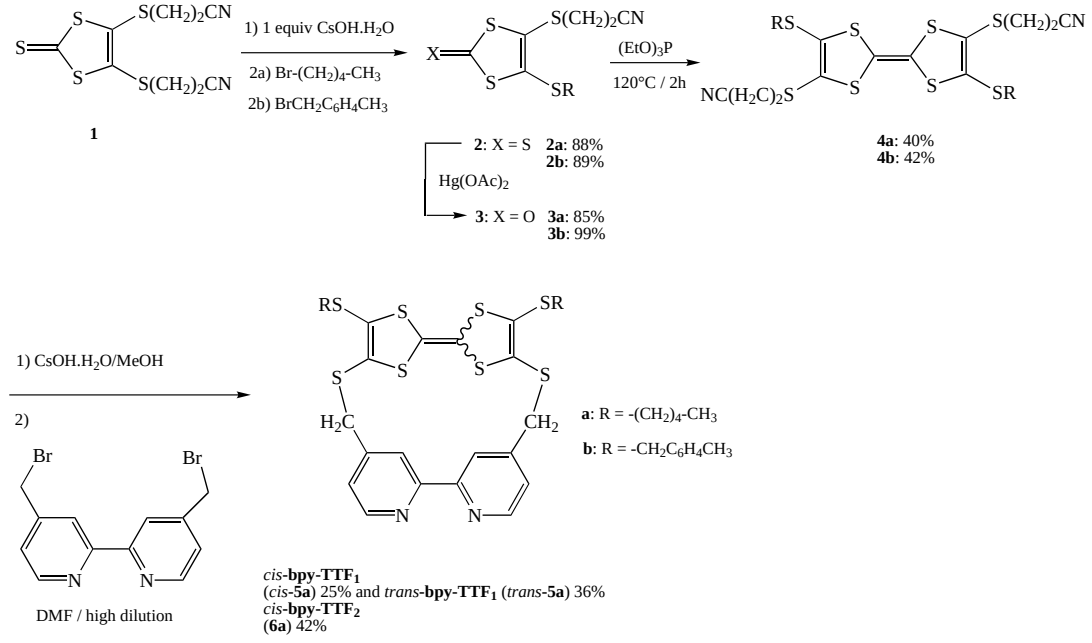

Scheme 2. Synthesis of bpy-TTF_1 and bpy-TTF_2.

0947-6539/02/0819-4462 $ 20.00+.50/0 *Chem. Eur. J.* **2002**, *8*, No. 19

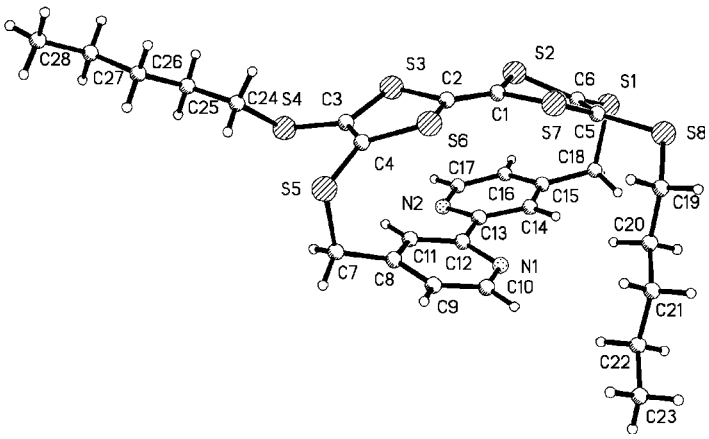

Figure 1. Molecular structure of *trans*-bpy-TTF_1.

Table 1. Redox data.[a]

Compound	$E_{1/2}$(ox)[b] [V]	$E_{1/2}$(red)[b] [V]
$[(bpy)_2Ru(bpy\text{-}TTF_1)]^{2+}$ (**7**)	+0.77 [1]; +0.90 [1]; +1.33 [1]	−1.31 [1][c]
$[(bpy)_2Ru(bpy\text{-}TTF_2)]^{2+}$ (**8**)	+0.79 [1]; +0.91 [1]; +1.32 [1]	−1.31 [1][c]
$[\{(bpy)_2Ru(\mu\text{-}2,3\text{-}dpp)\}_2Ru(bpy\text{-}TTF_1)]^{6+}$ (**9**)	+0.78 [1]; +0.90 [1]; +1.57 [2]	−0.55 [1]; −0.70 [1][c]
$[\{(bpy)_2Ru(\mu\text{-}2,3\text{-}dpp)\}_2Ru(bpy\text{-}TTF_2)]^{6+}$ (**10**)	+0.79 [1]; +0.91 [1]; +1.58 [2]	−0.55 [1]; −0.71 [1][c]
bpy-TTF_1	+0.64 [1]; +1.03 [1]	–
bpy-TTF_2	+0.63 [1]; +1.01 [1]	–
$[(bpy)_2Ru(4,4\text{-}Mebpy)]^{2+}$	+1.23 [1]	−1.30 [1][c]
$[\{(bpy)_2Ru(\mu\text{-}2,3\text{-}dpp)\}_2Ru(bpy)]^{6+}$	+1.51 [2]; +1.95 [1]	−0.52 [1]; −0.66 [1][c]

[a] Acetonitrile solution, room temperature. The number of exchanged electrons is given in brackets. [b] Versus SCE. [c] Successive reduction processes take place at more negative potentials, but they are not reported here because they are not necessary to the discussion.

components of the structure by comparison with the redox properties of the reference compounds bpy-TTF_1, bpy-TTF_2, $[Ru(bpy)_2(4,4'\text{-}Mebpy)]^{2+}$ (4,4′-Mebpy = 4,4′-dimethyl-2,2′-bipyridine),[8] and $[\{(bpy)_2Ru(\mu\text{-}2,3\text{-}dpp)\}_2Ru(bpy)]^{6+}$ [5a, c, 9] (Table 1). The first two one-electron oxidation processes in **7**–**10** can be assigned to the TTF subunits. The third process, one-electron in **7** and **8** and two-electron in **9** and **10**, is assigned to the metal centers. In particular, the two-electron process of **9** and **10** involve the two peripheral metal atoms of each compound.[3c] The first reduction processes are assigned to the 2,3-dpp bridging ligands in **9** and **10** and to an unsubstituted bpy ligand in **7** and **8**. The electron-donor substituents of bpy-TTF_1 and bpy-TTF_2 destabilize the π* orbitals of the bpy ligands and make reduction processes centered on the substituted ligands more difficult. Furthermore, the redox data indicate that the interaction between the redox-active sites is weak from an electrochemical viewpoint, since the changes in the redox potentials of the subunits in **7**–**10** relative to the model compounds are moderate (Table 1).

The absorption spectra of the compounds (Table 2, Figure 2) show features which are readily attributable to the individual components.[5, 8] The spectra are dominated by spin-allowed metal-to-ligand charge-transfer (MLCT) bands in the visible and by spin-allowed ligand-centered (LC) bands in the UV region.[5, 8] In particular, in the trinuclear complexes **9** and **10** the visible band around 436 nm is due to Ru → bpy CT transitions, and the broad band around 550 nm has contributions from $(bpy)_2Ru \rightarrow \mu$-2,3-dpp and (TTF-bpy)Ru → μ-2,3-dpp CT transitions. The main difference between **9** and **10** is the presence of a band at around 250 nm for **10**, also present in **8** but absent in **7**, due to transitions involving the phenyl ring of bpy-TTF_2.

The luminescence properties of **7**–**10** in acetonitrile at room temperature are very different from those of the parent complexes $[Ru(bpy)_2(4,4'\text{-}Mebpy)]^{2+}$ and $[\{(bpy)_2Ru(\mu\text{-}2,3\text{-}dpp)\}_2Ru(bpy)]^{6+}$ without TTF moieties: **7** and **8** exhibit emissions which, although spectrally close, are substantially reduced in lifetime relative to that of $[Ru(bpy)_2(4,4'\text{-}Mebpy)]^{2+}$ (Table 2), whereas **9** and **10** do not exhibit any detectable emission. The spectral similarity of the luminescence of the model compound $[Ru(bpy)_2(4,4'\text{-}Mebpy)]^{2+}$ with those of **7** and **8** suggests that the excited state responsible for the emission is identical in all cases, and is the ^{3}MLCT involving bpy as acceptor ligand.

To rationalize the strong emission quenching observed in **7** and **8**, reductive electron transfer involving the electron-donor TTF moieties can be considered (Figure 3, bottom). In a first approximation (neglecting the entropy factor and the work term), Equation (1)[10] allows the driving force ΔG_0 for reductive electron transfer from the TTF moieties to the excited metal-based chromophore(s) to be calculated.

$$\Delta G_0 = e(E_{ox} - {}^*E_{red}) \quad (1)$$

Here E_{ox} is the oxidation potential of the electron donor subunit (the TTF groups), $^*E_{red}$ is reduction potential of the excited state of the chromophore, which in turn is calculated

Table 2. Spectroscopic and photophysical data.[a]

Compound	Absorption	Luminescence	
	λ_{max} [nm] (ε [$M^{-1}cm^{-1}$])	298 K λ_{max} [nm] (τ [ns])	77 K[b] λ_{max} [nm] (τ [μs])
$[(bpy)_2Ru(bpy\text{-}TTF_1)]^{2+}$ (**7**)	285 (145300); 455 (18000)	620 (<1)	592 (5.3)
$[(bpy)_2Ru(bpy\text{-}TTF_2)]^{2+}$ (**8**)	286 (103700); 455 (17900)	620 (< 1)	592 (5.4)
$[\{(bpy)_2Ru(\mu\text{-}2,3\text{-}dpp)\}_2Ru(bpy\text{-}TTF_1)]^{6+}$ (**9**)	283 (176500); 436 (38400); 557 (38500)	no emission	727 (2.8)
$[\{(bpy)_2Ru(\mu\text{-}2,3\text{-}dpp)\}_2Ru(bpy\text{-}TTF_2)]^{6+}$ (**10**)	285 (199700); 435 (37200); 556 (39700)	no emission	724 (2.9)
$[(bpy)_2Ru(4,4\text{-}Mebpy)]^{2+}$	450 (16000)	620 (900)	592 (5.2)
$[\{(bpy)_2Ru(\mu\text{-}2,3\text{-}dpp)\}_2Ru(bpy)]^{6+}$	545 (28500)	804 (75)	721 (2.0)

[a] In deoxygenated acetonitrile solution, unless otherwise stated. [b] In butyronitrile rigid matrix.

  0947-6539/02/0819-4463 $ 20.00+.50/0

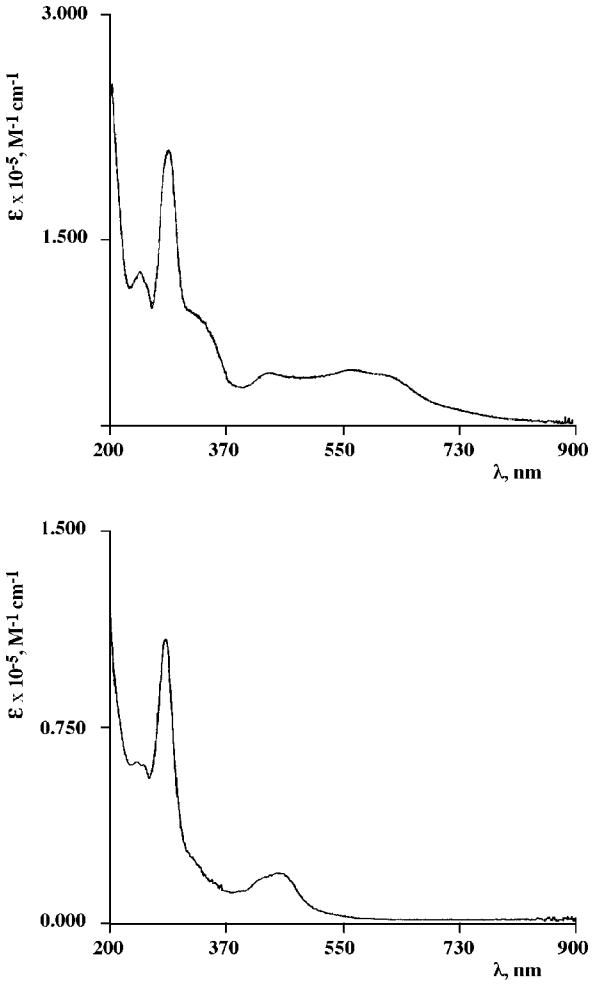

Figure 2. Absorption spectra of **10** (top) and **8** (bottom) in acetonitrile.

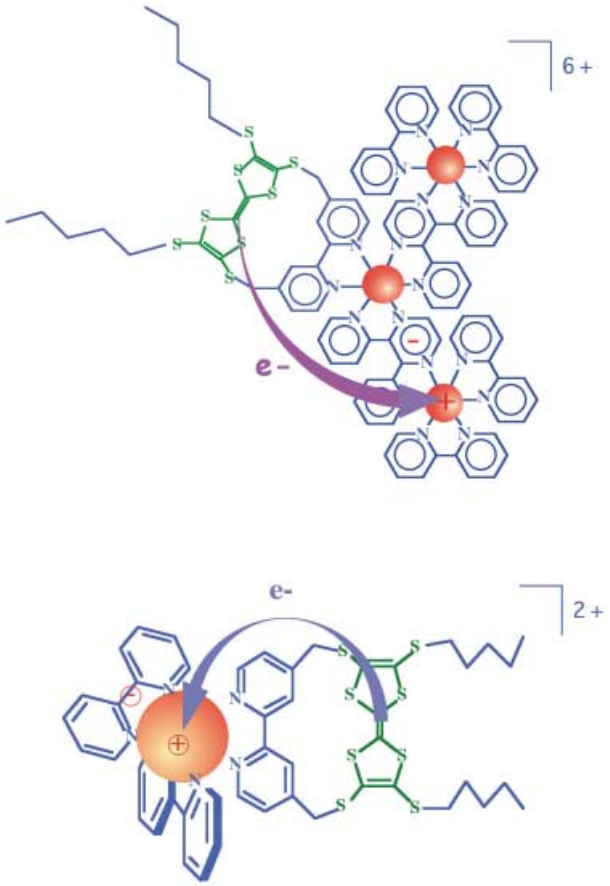

Figure 3. Representation of the electron-transfer processes in trinuclear (top) and mononuclear (bottom) complexes. The plus and minus mark the locations of the hole and the odd electron in the MLCT excited states before electron transfer (see text).

by the equation $^{*}E_{red} = E_{red} - E_{00}$, where E_{00} is the excited-state energy, taken as the highest energy feature of the 77 K emission spectrum. In the case of **7** and **8**, this driving force is around 0 eV, and this indicates that the charge-separated state produced by electron transfer is approximately isoenergetic with the luminescent Ru → bpy CT level(s). Since no alternative deactivation processes can be envisaged to explain the quenching of the MLCT emission **7** and **8** as opposed to their common model, we suggest that electron transfer from TTF to the excited Ru-based chromophore takes place in **7** and **8**. Further support for this hypothesis is provided by emission properties at 77 K (vide infra).

The absence of luminescence at room temperature for **9** and **10** suggests that electron transfer from the TTF moieties could also take place in these complexes (Figure 3, top). The luminescence of the model compound $[\{(bpy)_2Ru(\mu\text{-}2,3\text{-}dpp)\}_2Ru(bpy)]^{6+}$ originates from a triplet MLCT level involving the peripheral metal atom(s) and the bridging ligand,[5a,c] which is the lowest energy state of the multichromophore trinuclear array. The MLCT levels involving the central metal atom are deactivated by quantitative energy transfer to the peripheral chromophore(s).[5] The driving force for deactivation of the peripheral, emitting chromophores of the trinuclear Ru^{II} subunit by electron transfer from TTF moieties can be estimated by Equation (1), which yields a value of about −0.4 eV for this process. Figure 4 depicts the levels and decay processes involved. This indicates that the

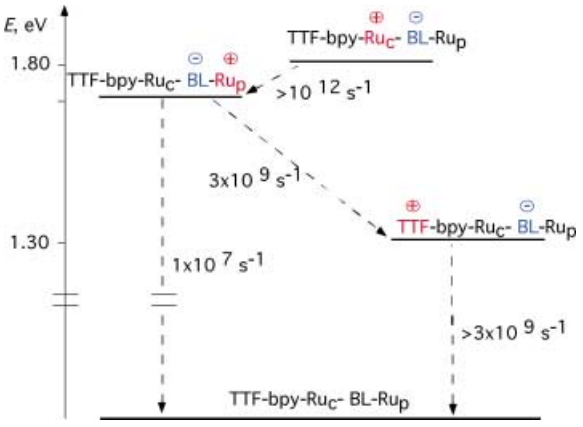

Figure 4. Schematic of the energy-level diagram and decay processes in the trinuclear species studied here. For simplicity reasons, the charges on the complexes are disregarded and only one "arm" of the trinuclear metal complex is represented. Ru_c and Ru_p indicate central and peripheral ruthenium centers, respectively. The location of the hole (⊕) and odd electron (⊖) of the MLCT and charge-separated states are marked, and the corresponding subunits are accordingly colored.

0947-6539/02/0819-4464 $ 20.00+.50/0 *Chem. Eur. J.* **2002**, *8*, No. 19

electron-transfer quenching in the trinuclear complexes is a thermodynamically allowed process and is therefore quite probable.

Time-resolved transient absorption spectroscopy allowed us to study the excited-state processes in more detail. We performed experiments on **7** and **9** in acetonitrile at room temperature; in both cases, the transient spectra were qualitatively identical to those of the corresponding model compounds. In particular, the transient absorption spectrum of **9** shows a bleaching around 540 nm, the region of the MLCT bands involving the bridging ligands, as expected for the lowest lying MLCT state of the trinuclear chromophore, and a transient absorption around 450 nm (Figure 5). Such

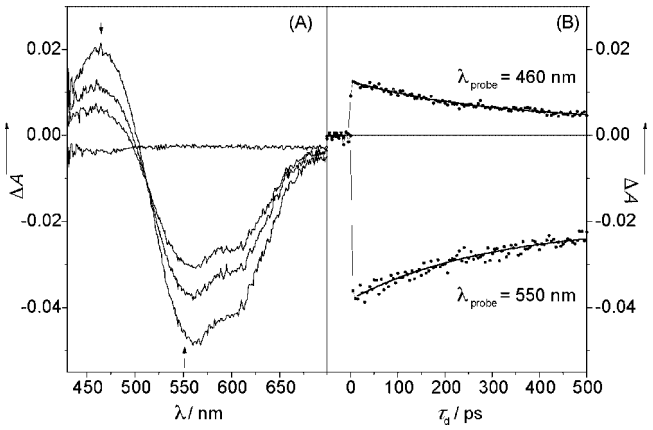

Figure 5. A) Transient difference absorption spectra of **9** in acetonitrile at room temperature, measured before the pulse (baseline) and at time delays of 0, 100, and 200 ps respectively, after 350 nm, 130 fs FWHM excitation. B) Kinetic profile of the difference absorbance of **9** in acetonitrile at room temperature probed at 460 nm and 550 nm, after 350 nm, 130 fs FWHM excitation.

bands for compound **9** decay in 300 ps with monoexponential kinetics, while the model trinuclear complex has a decay time of 70 ns. The decay of the transient spectrum of the model compound almost coincides with the luminescence lifetime of the same species (Table 2), while the transient absorption decay of **9** is in agreement with the MLCT emission quenching suggested by the luminescence experiments. The electron transfer from the TTF moiety to the excited (peripheral) chromophore is probably the origin of the excited-state quenching. From the decays of the transient spectra, a rate constant of $3 \times 10^9\ s^{-1}$ for such an electron transfer can be calculated,[11] and this value is reasonable for moderately exoergonic long-range electron-transfer processes.[3]

Unfortunately, there is no evidence of formation of oxidized TTF, which was expected to be indicated by a transient absorption around 700 nm.[12] This can be justified by assuming that in **9** the back electron transfer is faster than the forward electron transfer, so that the charge-separated state does not accumulate and cannot give rise to a detectable absorption. Indeed the forward and back electron-transfer processes involve different subunits: forward electron transfer takes place from the TTF moiety to a peripheral ruthenium center, that is, a metal ion other than that to which the TTF-substituted bpy ligand is coordinated, whereas the back-process involves the same TTF moiety and the bridging ligand, on which the excited electron is localized.[5] Therefore, the donor–acceptor distance is shorter, and the electronic coupling larger, for the back-process. The driving forces of the two processes are quite different, and that for the back-process of about -1.3 eV greatly exceeds that of the forward process (-0.4 eV, see above). It is conceivable that back electron transfer occurs in the Marcus-inverted region, and the recombination rate is thus slowed down, but the reorganization energy of the process is probably large enough to maintain the process in the normal region, so that the rate constant of the back-process remains higher than $3 \times 10^9\ s^{-1}$.

The transient absorption spectrum of the mononuclear complex **7** also shows features which can be assigned to lowest lying MLCT state(s). In particular, the MLCT band around 450 nm is strongly bleached. The transient spectrum decays in 500 ps[13] and gives a rate constant of $2 \times 10^9\ s^{-1}$ for the electron-transfer quenching process, which is slightly slower than that of **9** (see above). This result is expected if the different driving forces and donor–acceptor distances are taken into account; in **7** electron transfer involves the metal center and the TTF moiety, which are only separated by the coordinated bpy moiety of the bpy-TTF_1 ligand (ca. 6 Å from CPK models). This short donor–acceptor distance, which should lead to a faster rate for electron transfer in **7** than in **9**, is most likely counterbalanced by a very small driving force (see above). Also, in the case of **7** the oxidized TTF, and therefore the charge-separated state, is not evidenced in the transient spectrum, and this suggests that for the mononuclear complex the back electron transfer is also faster than the forward process.

In contrast to the situation at room temperature, the luminescence properties of **7**–**10** at 77 K in a rigid butyronitrile matrix are very similar to those of the corresponding parent compounds without the TTF electron donor groups, $[Ru(bpy)_2(4,4'\text{-Mebpy})]^{2+}$ and $[\{(bpy)_2Ru(\mu\text{-}2,3\text{-dpp})\}_2Ru(bpy)]^{6+}$ (Table 2). Clearly the TTF subunits do not affect the properties of the Ru-based chromophores under these experimental conditions. This finding strongly supports the assignment of the emission quenching at room temperature to electron-transfer processes. It is well known that electron transfer can be strongly slowed down in a rigid matrix at 77 K, because of the presence of significant nuclear barriers and destabilization of the charge-separated state.[3, 9a, 14]

Finally, the decay processes taking place in the antenna moieties of **9** and **10** at room temperature deserve further comment. Although the central Ru-based chromophore in the model compound $[\{(bpy)_2Ru(\mu\text{-}2,3\text{-dpp})\}_2Ru(bpy)]^{6+}$ is deactivated quantitatively by energy transfer to the peripheral ones (see above),[5] in **9** and **10** it could in principle be directly quenched through electron transfer by the TTF subunit before energy transfer occurs. Indeed, this process is even more thermodynamically allowed than electron transfer involving the peripheral Ru-based chromophores. However, it was demonstrated recently that in dinuclear[15] and tetranuclear[16] Ru^{II} and Os^{II} complexes with bridging 2,3-dpp ligands, energy transfer between neighboring chromophores is faster than 200 fs (this also implies the occurrence of singlet–singlet energy transfer), even in the presence of small driving

  0947-6539/02/0819-4465 $ 20.00+.50/0

forces. Hence, it is reasonable to assume that energy transfer from MLCT states involving the central Ru^{II} center to MLCT states involving the peripheral Ru-based chromophores in **9** and **10** also takes place on such a timescale (i.e., faster than 200 fs). Direct electron transfer from TTF moieties to the excited central Ru chromophore of the trinuclear antenna subunit is a similar process to the electron-transfer quenching occurring in **7** and **8**, but with a significantly larger driving force. Therefore, a faster rate than that calculated for the quenching process in **7** ($2 \times 10^9\,s^{-1}$) is predicted for reductive electron transfer involving the central chromophore of **9** and **10**. However, it is hard to foresee that this electron transfer can be three orders of magnitude faster than the analogous process in **7**, and therefore we assume that it cannot compete with the ultrafast energy transfer within the antenna. In conclusion, even in the absence of direct evidence, and on the basis of the rates of the intercomponent energy transfer processes taking place in this type of multichromophore system,[15] we propose that energy transfer within the antenna trinuclear system preceeds the charge-separation process.

Conclusion

The results obtained for compounds **9** and **10** are interesting from a number of viewpoints. First, the metal atom to which the quencher subunit is connected is not involved in the quenched MLCT level. To the best of our knowledge, this is the first reported case of this behavior, and implies the occurrence of long-range electron transfer, probably mediated by a superexchange mechanism.[17, 18] Second, the coupling of the trinuclear compound $[\{(bpy)_2Ru(\mu\text{-}2,3\text{-}dpp)\}_2Ru(bpy)]^{6+}$, which can be regarded as a small antenna since it is a multichromophore species in which fast energy-transfer processes take place within the components, with the electron donors TTF_1 and TTF_2 has been achieved. The fast energy-transfer processes in the trimetallic subunit, together with the efficiency of the electron-transfer quenching of the emission of the trinuclear complex by TTF moieties, demonstrate that we have prepared the first functional antenna/reaction center system involving metal complexes.[4, 19]

Note that in **9** and **10** the luminescence of the entire array is quenched, although the redox-active quencher is not directly connected to the lowest energy chromophore(s) of the antenna (the so-called energy traps). This observation may be important for future design of functional antenna/reaction center assemblies and suggests that, at least in some cases, it is not strictly necessary to directly connect the charge-separation subunit to the antenna energy trap.

Experimental Section

General: All reactions were carried out under an atmosphere of dry N_2 unless otherwise stated. THF was distilled from Na/benzophenone immediately prior to use; toluene was also purified by this procedure when high purity was needed. MeOH was distilled from Mg. DMF and CH_3CN were allowed to stand over molecular sieves (4 Å) for at least three days before use. Triethylphosphite was purified by distillation and stored over molecular sieves (3 Å). All reagents were standard grade and used as received. 4,5-Bis(2-cyanoethylthio)-1,3-dithiol-2-thione[7] and 4,5-bis(2-cyanoethylthio)-1,3-dithiol-2-one[7] were prepared according to literature procedures.

Analytical TLC was performed on Merck DC-Alufolien Kieselgel 60 F_{254} 0.2 mm thickness precoated TLC plates, and column chromatography on Merck Kieselgel 60 (0.040/0.063 mm, 230/400 mesh AST0000M). Melting points are uncorrected. ^1H NMR spectra were recorded at 300 or 250 MHz; ^{13}C NMR spectra were recorded at 75 or 63 MHz with broad-band decoupling. Plasma desorption mass spectrometry (PDMS) was carried out on a Bio-Ion 20R time-of-flight instrument. Electron impact (EI) mass spectra were recorded on a Varian MAT 311A triple-quadropole instrument, and Fast Atom Bombardment (FAB) mass spectra were recorded on a Kratos MS 50 TC instrument.

4-(2′-Cyanoethylthio)-5-pentylthio-1,3-dithiol-2-thione (2a): A solution of $CsOH \cdot H_2O$ (2.66 g, 15.8 mmol) in degassed MeOH (75 mL) was slowly added (2.5 h) to a solution of 4,5-bis-(2-cyanoethylthio)-2-thione-1,3-dithiole[7] (5.75 g, 18.9 mmol) in CH_3CN (500 mL). After stirring for an additional 30 min, a solution of bromopentane (2.25 mL, 18 mmol) in MeOH (5 mL) was added, and the mixture stirred overnight, followed by concentration in vacuo, washing with water, and extraction of the residual oil into CH_2Cl_2. Evaporation in vacuo and column chromatography (SiO_2, petroleum ether/CH_2Cl_2 20/80) yielded two fractions. The second fraction yielded the title compound **2a** as a yellow oil. Yield: 5.30 g, 87 %; ^1H NMR (200 MHz, $CDCl_3$): $\delta = 0.91$ (t, 3H; CH_3), 1.37 (m, 4H; $(CH_2)_2CH_3$), 1.69 (m, 2H; SCH_2CH_2), 2.75 (t, 2H; SCH_2CH_2CN), 2.93 (t, 2H; $SCH_2(CH_2)_3CH_3$), 3.l0 (t, 2H; SCH_2CH_2CN); ^{13}C NMR: $\delta = 13.96$, 18.88, 22.18, 29.41, 30.68, 32.02, 36.75, 117.35, 128.91, 143.49, 211.13; MS (IE): *m*/*z* (%): 321 (100), 198 (61), 191 (25), 88 (33); calcd: $C_{11}H_{15}NS_5$ (321.50).

4-(2′-Cyanoethylthio)-5-pentylthio-1,3-dithiol-2-one (3a): $Hg(OAc)_2$ (9.35 g, 29.5 mmol) was added to a solution of **2a** (3.78 g, 12 mmol) in $CHCl_3$ (90 mL) and glacial acetic acid (30 mL) under N_2. After stirring overnight the white reaction mixture was filtered through Celite. The filtrate was treated with saturated $NaHCO_3$ (75 mL) and water (150 mL), dried (Na_2SO_4), and concentrated in vacuo. After column chromatography (SiO_2, CH_2Cl_2) **3a** was obtained as a yellow oil. Yield: 3.40 g (95 %); ^1H NMR (200 MHz, $CDCl_3$): $\delta = 0.93$ (m, 3H; CH_3), 1.39 (m, 4H; $(CH_2)_2CH_3$), 1.67 (m, 2H; SCH_2CH_2), 2.73 (m, 2H; SCH_2CH_2CN), 2.90 (m, 2H; SCH_2), 3.08 (m, 2H; SCH_2CH_2CN); ^{13}C NMR ($CDCl_3$): $\delta = 13.94$, 18.26, 21.66, 28.87, 30.15, 31.35, 36.25, 120.46, 133.43, 188.77; MS (IE): *m*/*z* (%): 305 (98), 213 (18), 147 (39), 130 (30), 70 (100); calcd: $C_{11}H_{11}NOS_4$ (305.51).

4-(2′-Cyanoethylthio)-5-(4-methylbenzylthio)-1,3-dithiol-2-thione (2b) was prepared by the procedure described above for **2a**. $CsOH \cdot H_2O$ (3.47 g, 20.69 mmol) in dry MeOH (100 mL) was added to 4,5-bis(2-cyanoethylthio)-1,3-dithiol-2-thione (6.00 g, 19.7 mmol) in dry DMF (100 mL) under N_2 over 60 min. Stirring was continued for 30 min, whereupon *p*-methylbenzylbromide (4.01 g, 21.7 mmol) in dry DMF (30 mL) was added in one portion, followed by stirring overnight. Concentration in vacuo, workup as above, and chromatography (SiO_2, CH_2Cl_2/cyclohexane 2/1) gave a yellow fraction, which was isolated and recrystallized to give **2b** as long yellow neddles. Yield: 6.20 g, 89 %; m.p. 91 – 92 °C; ^1H NMR ($CDCl_3$): $\delta = 2.36$ (s, 3H; CH_3), 2.43 (t, $J = 7.2$ Hz, 2H; SCH_2CH_2CN), 2.87 (t, $J = 7.2$ Hz, 2H; SCH_2CH_2CN), 4.06 (s, 2H; SCH_2Ph), 7.17 ppm (m, 4H; C_6H_4); ^{13}C NMR ($CDCl_3$): $\delta = 18.24$, 21.13, 31.81, 40.85, 117.03, 128.79, 129.56, 132.65, 138.14, 140.99, 210.36 ppm; MS (EI): *m*/*z* (%): 355 (11), 105 (100); elemental analysis (%) calcd for $C_{14}H_{13}NS_5$ (355.59): C 47.29, H 3.69, N 3.94, S 45.08; found: C 47.37, H 3.70, N 3.77, S 45.25.

4-(2′-Cyanoethylthio)-5-(4-methylbenzylthio)-1,3-dithiol-2-one (3b): $Hg(OAc)_2$ (11.95 g, 37.50 mmol) was added to a solution of **2b** (5.00 g, 14.1 mmol) in $CHCl_3$ (100 mL) and glacial acetic acid (50 mL) under N_2. This mixture was stirred overnight and then the white reaction mixture was filtered through Celite. The filtrate was treated with saturated $NaHCO_3$ (5×200 mL) and water (100 mL), dried (Na_2SO_4), and concentrated in vacuo to give **3b** as yellow crystals. Yield: 4.73 g (99 %); m.p. 49 – 50 °C; ^1H NMR ($CDCl_3$): $\delta = 2.36$ (s, 3H; CH_3), 2.45 (t, $J = 7.3$ Hz, 2H; SCH_2CH_2CN), 2.84 (t, $J = 7.3$ Hz, 2H; SCH_2CH_2CN), 4.03 (s, 2H; SCH_2Ph), 7.17 ppm (m, 4H; C_6H_4); ^{13}C NMR ($CDCl_3$): $\delta = 18.02$, 21.09, 31.59, 40.74, 117.16, 124.61, 128.78, 129.45, 131.93, 133.10, 137.95, 188.67 ppm; MS(EI): *m*/*z* (%): 339 (7), 105 (100); elemental analysis (%)

0947-6539/02/0819-4466 $ 20.00+.50/0 *Chem. Eur. J.* **2002**, *8*, No. 19

calcd for $C_{14}H_{13}NOS_4$ (339.52): C 49.53, H 3.86, N 4.13, S 37.77; found: C 49.62, H 3.81, N 4.02, S 37.93.

2,6(7)-Bis(cyanoethylthio)-3,7(6)-bis(pentylthio)tetrathiafulvalene (4a): A stirred suspension of **3a** (10 mmol) in distilled triethyl phosphite (20 mL) was heated for 2 h at 120 °C under N_2. Cooling, addition of MeOH, filtering, and washing the red precipitate with MeOH and drying gave the red title compound **4a** as a mixture of *cis* and *trans* isomers. Yield: 40 %; m.p. 98 °C; ^{1}H NMR (200 MHz, $CDCl_3$): $\delta = 0.92$ (t, 6H; CH_3), 1.38 (m, 8H; $(CH_2)_2CH_3$), 1.67 (q, 4H; SCH_2CH_2), 2.71 (t, 4H; SCH_2CH_2CN), 2.88 (t, 4H; SCH_2), 3.04 ppm (t, 4H; SCH_2CH_2CN); ^{13}C NMR ($CDCl_3$): $\delta =$ 13.97, 18.75, 22.19, 29.51, 30.67, 31.35, 36.46, 110.84, 122.42, 134.60 ppm; MS (FAB): *m/z* (%): 578 (100); elemental analysis (%) calcd for $C_{22}H_{30}S_8N_2$ (578.02): C 45.63, H 5.22, N 4.83; found: C 45.61, H 4.99, N 4.84.

2,6(7)-Bis(2-cyanoethylthio)-3,7(6)-(4-methylbenzylthio)-tetrathiafulvalene (4b): A stirred suspension of **3b** (4.20 g, 12.4 mmol) in distilled triethyl phosphite (20 mL) was heated at 120 °C for 90 min. Cooling (0 °C), addition of MeOH (150 mL), filtering, washing the precipitate with MeOH, and drying gave red **4b** as a mixture of *cis* and *trans* isomers. Yield: 3.34 g (84 %), m.p. 129–130 °C; ^{1}H NMR ($CDCl_3$): $\delta = 2.24$ (m, 4H; SCH_2CH_2CN), 2.37 (s, 6H; CH_3), 2.80 (m, 4H; SCH_2CH_2CN), 4.04 (s, 4H; SCH_2Ph), 7.19 ppm (m, 8H; C_6H_4); ^{13}C NMR ($CDCl_3$): $\delta = 17.85$, 21.12, 31.06, 40.34, 110.53, 117.8, 125.57, 128.83, 129.40, 132.46, 133.61, 137.72 ppm; MS (FAB): *m/z*: 646 $[M]^+$; CV (CH_2Cl_2, versus Ag/AgCl): $E_{1/2} = 0.65$, 0.99 V; elemental analysis (%) calcd for $C_{28}H_{26}N_2S_8$ (646.05): C 51.98, H 4.05, N 4.33, S 39.64; found: C 52.13, H 4.08, N 4.33, S 39.59.

***cis*- and *trans*-bpy-TTF$_1$ (*cis*- and *trans*-5a)**: Compound **4a** (1.216 g, 2.10 mmol) was dissolved in DMF (45 mL), and the solution degassed (N_2). Subsequent addition of a solution of $CsOH \cdot H_2O$ (0.741 g, 4.41 mmol) in dry MeOH (5 mL) resulted in a color change from orange to deep red that indicated formation of the bis-thiolate. This solution and a solution of 4,4′-bis(bromomethyl)-2,2′-bipyridine[7b] (0.718g, 2.10 mmol) in DMF (50 mL) were mixed by using a Perfusor pump (addition speed 2.7 mL/h). The resulting mixture was concentrated in vacuo and redissolved in CH_2Cl_2 (300 mL). The organic phase was then treated with water (300 mL), saturated aqueous NaCl (2 × 300 mL), and water (300 mL), dried (Na_2SO_4), and concentrated in vacuo. The crude product was treated with a mixture of CH_2Cl_2 (19 mL) and MeOH (6.5 mL) and left in the freezer for 24 h, and the resulting yellow precipitate was isolated and recrystallized from absolute EtOH or $CNCH_3$. This gave pure *cis*-**5a** as fine yellow neddles. Column chromatography of the filtrate (SiO_2, ethyl acetate) gave in the first fraction *trans*-**5a** followed by a small fraction of the *cis* isomer.

***cis*-5a**: Yield: 0.349 g (0.534 mmol, 25 %), m.p. 134–135 °C; ^{1}H NMR ($CDCl_3$): $\delta = 0.89$ (t, $J = 6.9$ Hz, 6H; CH_2CH_3), 1.32 (m, 8H; $CH_2CH_2CH_2CH_3$), 1.46 (m, 4H; SCH_2CH_2), 2.59 (t, $J = 7.3$ Hz, 4H; $SCH_2C_4H_9$), 4.02 (s, 4H; SCH_2Py), 7.34 (dd, $J = 1.5$, 5.0 Hz, 2H; Py*H*-5,5′), 7.99 (s, 2H; Py*H*-3,3′), 8.74 ppm (d, $J = 5.0$ Hz, 2H; Py*H*-6,6′); ^{13}C NMR ($CDCl_3$): $\delta = 13.79$, 21.97, 28.89, 30.46, 36.78, 38.74, 115.11, 121.03, 123.09, 123.96, 134.80, 146.18, 150.71, 154.82 ppm; MS (FAB): *m/z*: 652 $[M]^+$; PDMS: *m/z* (%): 652 (100); CV (CH_2Cl_2, versus Ag/AgCl): $E_{1/2} = 0.64$, 1.05 V; elemental analysis (%) calcd for $C_{28}H_{32}N_2S_8$ (353.10): C 51.50, H 4.94, N 4.29, S 39.27; found: C 51.55, H 4.35, N 4.35, S 39.12.

***trans*-5a**: Yield: 0.490 g (0.750 mmol, 36 %); m.p. 130–131 °C; ^{1}H NMR ($CDCl_3$): $\delta = 0.92$ (t, $J = 7.1$ Hz, 6H; CH_2CH_3), 1.38 (m, 8H; $CH_2CH_2CH_2CH_3$), 1.67 (m, 4H; SCH_2CH_2), 2.85 (m, 4H; $SCH_2C_4H_9$), 3.84 (d, $J = 11.9$ Hz, 2H; SCH_2Py), 4.10 (d, $J = 11.9$ Hz, 2H; SCH_2Py), 7.36 (dd, $J = 1.5$, 5.1 Hz, 2H; Py*H*-5,5′), 7.55 (d, $J = 1.5$ Hz, 2H; Py*H*-3,3′), 8.62 ppm (d, $J = 5.1$ Hz, 2H; Py*H*-6,6′); ^{13}C NMR ($CDCl_3$): $\delta = 13.85$, 21.98, 29.45, 30.63, 36.24, 37.89, 115.10, 118.11, 122.72, 124.31, 137.87, 145.99, 149.76, 156.65 ppm; MS (FAB): *m/z*: 652 $[M]^+$; PDMS: *m/z*: (%): 652 (100); CV (CH_2Cl_2, versus Ag/AgCl): $E_{1/2} = 0.63$, 1.04 V; elemental analysis (%) found: C 51.55, H 5.00, N 4.35, S 39.12.

***cis*-bpy-TTF$_2$ (*cis*-6a)**: $CsOH \cdot H_2O$ (0.282 g, 1.679 mmol) in dry MeOH (10 mL) was slowly added (20 min) to a solution of **4b** (0.518 g, 0.801 mmol) in dry DMF (80 mL) under N_2, and the mixture stirred (20 min). Then 4,4′-bis(bromomethyl)-2,2′-bipyridine[7b] (0.274 g, 0.801 mmol) in dry DMF (20 mL) was added in one portion, and the mixture stirred overnight. The mixture was concentrated in vacuo, dissolved in CH_2Cl_2 (200 mL), and extracted with water (200 mL) and saturated aqueous NaCl (2 × 300 mL). After drying (Na_2SO_4) and concentration in vacuo, the residue was redissolved in CH_2Cl_2 (10 mL), and MeOH (10 mL) was added. The title product precipitated as yellow crystals after storage (24 h) at −20 °C. Recrystallization gave pure *cis*-**6a** as yellow neddles. Yield: 0.242 g (42 %); m.p. 104–105 °C; ^{1}H NMR ($CDCl_3$): $\delta =$ 2.33 (s, 6H; CH_3), 3.76 (s, 4H; SCH_2Ph), 3.98 (s, 4H; SCH_2Py), 7.13 (m, 8H; C_6H_4), 7.37 (d, $J = 4.9$ Hz, 2H; Py*H*-5,5′), 7.98 (s, 2H; Py*H*-3,3′), 8.77 ppm (d, $J = 4.9$ Hz, 2H; Py*H*-6,6′); ^{13}C NMR ($CDCl_3$): $\delta = 21.18$, 38.95, 41.37, 114.94, 123.03, 123.09, 123.89, 128.91, 129.38, 132.71, 133.99, 137.49, 146.14, 150.52, 154.73 ppm; MS(PDMS): *m/z*: 723 (calcd 720); CV (CH_2Cl_2, versus Ag/AgCl): $E_{1/2} = 0.65$, 1.04 V; elemental analysis (%) calcd for $C_{34}H_{28}N_2S_8$ (721.13): C 56.63, H 3.91, N 3.89, S 35.57; found: C 56.37, H 4.03, N 3.97, S 35.67.

[(bpy-TTF$_1$)Ru(bpy)$_2$](PF$_6$)$_2$ (7): $[RuCl_2(bpy)_2]$ (50 mg, 0.103 mmol) in ethanol (10 mL) was refluxed for 6 h. Then *cis*-bpy-TTF$_1$ (101 mg, 0.154 mmol) was added, and the mixture refluxed for 18 h.[20] The cooled solution was treated with an excess of solid NH_4PF_6, and the resulting brown precipitate was isolated by filtration and purified by column chromatography on neutral aluminum oxide (∅ 2.5 cm, length 20 cm; aluminum oxide activity 1) with CH_2Cl_2/MeOH (9/1) as eluent. The first band obtained (dark orange) was rotary evaporated, and the residue dissolved in a small amount of CH_3CN and precipitated by addition of diethyl ether. The final product was a violet solid (55 %). Elemental analysis (%) calcd for $C_{47}H_{48}N_6S_8RuP_2F_{12}$: C 41.96, H 3.60, N 6.25, S 19.03; found C 41.82, H 3.48, N 6.12, S 19.44. TOF-SIMS: *m/z*: 1199; calcd for $[M - PF_6]^+$: 1199.

[(bpy-TTF$_2$)Ru(bpy)$_2$](PF$_6$)$_2$ (8): $[RuCl_2(bpy)_2]$ (50 mg, 0.103 mmol) in ethanol (10 mL) was refluxed for 6 h. Then *cis*-bpy-TTF$_2$ (111 mg, 0.154 mmol), was added and the mixture refluxed for 15 h. The cooled solution was treated with an excess of solid NH_4PF_6, and the brown precipitate formed was isolated by filtration and purified by column chromatography on neutral aluminum oxide (∅ 2.5 cm, length 20 cm, aluminum oxide activity 1) by eluting with CH_2Cl_2/MeOH (9/1). The first band obtained (dark orange), was rotary evaporated, and the residue dissolved in a small amount of CH_3CN and precipitated by addition of diethyl ether. The final product was a violet solid (63 %). Elemental analysis (%) calcd for $C_{53}H_{44}N_6S_8RuP_2F_{12}$: C 45.05, H 3.14, N 5.95, S 18.11; found C 45.60, H 3.28, N 5.82, S 17.98. TOF-SIMS: *m/z*: 1267; calcd for $[M - PF_6]^+$: 1266.

[(bpy-TTF$_1$)Ru{(μ-2,3-dpp)Ru(bpy)$_2$}$_2$](PF$_6$)$_6$ (9): A mixture of $[Cl_2Ru\{(\mu\text{-}2,3\text{-dpp})Ru(bpy)_2\}_2](PF_6)_4$ (50 mg, 0.034 mmol) and $AgNO_3$ in ethanol (10 mL) was refluxed for 12 h. This solution was added slowly to a solution of *cis*-bpy-TTF$_1$ (33 mg, 0.051 mmol) in ethanol (5 mL), and the mixture was refluxed for 24 h.[17] The cooled solution was treated with an excess of solid NH_4PF_6, and the violet precipitate formed was isolated by filtration and purified by column chromatography on neutral aluminum oxide (∅ 2.5 cm, length 20 cm, aluminum oxide activity 1) by eluting with CH_2Cl_2/MeOH (9/1). The second band obtained (violet), was rotary evaporated, and the residue dissolved in a small amount of CH_3CN and precipitated by addition of diethyl ether. The final product was a violet solid (60 %). Elemental analysis (%) calcd for $C_{93}H_{84}N_{18}S_8Ru_3P_6F_{36}$: C 38.70, H 2.94, N 8.74, S 8.87; found C 38.95, H 3.06, N 8.72, S 8.61. TOF-SIMS: *m/z*: 2738; calcd for $[M - PF_6]^+$: 2739.

[(bpy-TTF$_2$)Ru{(μ-2,3-dpp)Ru(bpy)$_2$}$_2$](PF$_6$)$_6$ (10): A mixture of $[Cl_2Ru\{(\mu\text{-}2,3\text{-dpp})Ru(bpy)_2\}_2](PF_6)_4$ (50 mg, 0.034 mmol) and $AgNO_3$ in ethanol (10 mL) was refluxed for 12 h. The solution was added slowly to a solution of *cis*-bpy-TTF$_2$ (37 mg, 0.051 mmol) in ethanol (5 mL), and the mixture refluxed for 22 h. The cooled solution was treated with an excess of solid NH_4PF_6, and the violet precipitate formed was isolated by filtration and purified by column chromatography on neutral aluminum oxide (∅ 2.5 cm, length 20 cm, aluminum oxide activity 1) by eluting with CH_2Cl_2/MeOH (9/1). The second band obtained (violet) was rotary evaporated, and the residue dissolved in a small amount of CH_3CN and precipitated by addition of diethyl ether. The final product was a violet solid (65 %). Elemental analysis (%) calcd for $C_{99}H_{80}N_{18}S_8Ru_3P_6F_{36}$: C 40.24, H 2.73, N 8.54, S 8.66; found C 40.51, H 2.80, N 8.55, S 8.52. TOF-SIMS: *m/z*: 2807; calcd for $[M - PF_6]^+$: 2807.

Determination of spectroscopic, photophysical, and redox properties: Electronic absorption spectra were recorded on an HP 8453 spectrophotometer and on a Kontron Uvikon 860 spectrophotometer. For steady-state luminescence measurements, a Jobin Yvon-Spex Fluoromax 2 spectrofluorimeter was used, equipped with a Hamamatsu R3896 photomultiplier,

and the spectra were corrected for photomultiplier response by using a program purchased with the fluorimeter. For the luminescence lifetimes, an Edinburgh FL 900 single-photon-counting spectrometer was used.

The laser system employed for the ultrafast transient absorption spectrometry experiments is based on a Spectra-Physics Hurricane Titanium Sapphire regenerative amplifier system. The optical bench assembly of the Hurricane includes a seeding laser (Mai Tai), a pulse stretcher, a Ti:sapphire regenerative amplifier, a Q-switched pumped laser (Evolution), and a pulse compressor. The output of the laser is typically 1 mJ per pulse (130 fs FWHM) at a repetition rate of 1 kHz. Two different pump–probe setups were used (see Figure 6): 1) A full-spectrum setup based on an optical parametric amplifier (Spectra-Physics OPA 800) as pump. The fundamental light (2 μJ per pulse) was used for white-light generation, which was detected with a CCD spectrograph. 2) Single-wavelength kinetics measurements based on two OPAs, one of which was used as pump and the other as probe, and an amplified Si photodiode for detection. For both setups OPA(1) was used to generate excitation pulses at 350 nm (fourth harmonic of the 1400 nm OPA signal beam) and OPA(2) 460/550 nm (fourth harmonic of the 1840/2200 nm OPA idler beam). The output power was typically 4 μJ per pulse.

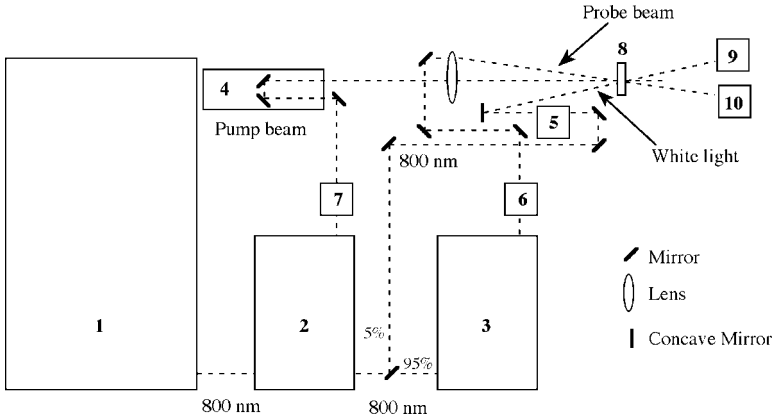

Figure 6. Schematic of the ultrafast spectrometer employed: 1) Hurricane. 2) OPA-800 (pump). 3) OPA-800 (probe). 4) Delay line. 5) White-light generator. 6) Berek polarizer. 7) Chopper. 8) Cell. 9) Detector (CCD). 10) Detector (Si photodiode).

The pump light was passed over a delay line (Physik Instrumente, M-531DD) that provides an experimental time window of 1.8 ns with a maximum resolution of 0.6 fs per step. The white light was generated by focusing the fundamental (800 nm) into a H_2O flow-through cell (10 mm, Hellma). For the single-wavelength measurements, the polarization of probe light was controlled by a Berek Polarization Compensator (New Focus). The energy of the probe pulses was about 5×10^{-3} μJ per pulse at the sample. The angle between the pump and probes beam was typically 5–7°. The circular cuvette ($d = 1.8$ cm, 1 mm; Hellma), with a solution of the sample, was placed in a homemade rotating ball bearing (1000 rmp) to avoid local heating by the laser beams.

For the white-light/CCD setup, the probe beam was coupled into 400 μm optical fiber after passing the sample and detected by a CCD spectrometer (Ocean Optics, PC2000). The chopper (Rofin Ltd., $f = 10$–20 Hz), placed in the excitation beam, provided I and I_0 according to its open or closed status. The excited-state spectra were obtained by $\Delta A = \lg(I/I_0)$. Typically, 2000 excitation pulses were averaged to obtain the transient at a particular time. A chirp of < 1 ps was observed between 425 and 700 nm. For the single-wavelength kinetic measurement, an amplified Si photodiode (NewPort, 818 UV/4832-C) was used. The output of the Si photodiode was connected to an AD converter (National Instruments, PCI 4451, 205 kS/s) that enabled us to measure the intensity of each separate pulse. Here, too, analogous to the white-light/CCD setup, the chopper ($f = 50$ Hz) placed in the excitation beam provided I, I_0, and ΔA. Typically, 500 excitation pulses were averaged to obtain the transient at a particular time.

The CCD spectrograph, chopper, Si photodiodes, AD converter and delay line were driven by a computer. In-house-developed LabVIEW (National Instruments) software routines were used for spectral acquisition and single-line measurements over a series of different delay settings. The total instrument rise time of the ultrafast spectrometer was about 300 fs. The solutions of the samples were prepared to have an optical density of about 0.8 at the excitation wavelength in a 1 mm cell. The absorbance spectra of the solutions were measured before and after the experiments. No photodecomposition was observed.

Electrochemical measurements were carried out in argon-purged acetonitrile at room temperature with a PAR 273 multipurpose device interfaced to a PC. The working electrode was a glassy carbon electrode (8 mm^2, Amel). The counterelectrode was a Pt wire, and the reference electrode was an SCE separated with a fine glass frit. The concentration of the complexes was about 5×10^{-4} M. Tetrabutylammonium hexafluorophosphate was used as supporting electrolyte (0.05 M). Cyclic voltammograms were obtained at scan rates of 20, 50, 200, and 500 mV s^{-1}. For reversible processes, half-wave potentials (versus SCE) were calculated as the average of the cathodic and anodic peaks. The criteria for reversibility were a separation of 60 mV between cathodic and anodic peaks, a ratio of the intensities of the cathodic and anodic currents close to unity, and the constancy of the peak potential on changing the scan rate. The number of exchanged electrons was measured in differential pulse voltammetry (DPV) experiments performed with a scan rate of 20 mV s^{-1}, a pulse height of 75 mV, and a duration of 40 ms, and by taking advantage of the presence of ferrocene used as the internal reference.

Experimental uncertainties were as follows: absorption maxima, ±2 nm; molar absorption coefficient, 10%; emission maxima, ±5 nm; excited state lifetimes, 10%; luminescence quantum yields, 20%; redox potentials, ± 10 mV.

Crystal structure analysis: Suitable crystals of *trans*-bpy-TTF_1 were produced by recrystallization from ethanol. $C_{28}H_{32}N_2S_8$, $M_r = 653.04$, triclinic, $a = 9.7468(19)$, $b = 12.094(2)$, $c = 14.758(3)$ Å, $\alpha = 66.42(3)$, $\beta = 79.32(3)$, $\gamma = 74.82(3)°$, $V = 1532.3(5)$ Å^3, space group $P\bar{1}$, $Z = 2$, $\rho_{calcd} = 1.415$ g cm^{-3}, $F(000) = 684$, graphite-monochromated $Mo_{K\alpha}$ radiation, $\lambda = 0.71073$ Å, $\mu = 0.605$ mm^{-1}, $T = 120$ K. Crystal dimensions $0.37 \times 0.24 \times 0.10$ mm; yellow prism. The intensities of 16216 reflections were measured on a Siemens/Bruker SMART 1K CCD diffractometer to $\theta_{max} = 26.36°$ and were merged to 6216 unique reflections ($R_{int} = 0.0184$). Data collection, integration of frame data, and conversion to intensities were performed by using the programs SMART[21] SAINT,[22] and SADABS.[23] Structure solution, refinement and analysis of the structure, and production of crystallographic illustrations were carried with the programs SHELXTL[24] and PLATON.[25] The refinement using 345 parameters converged at $R_1 = 0.0242$ (for $F_o > 4\sigma(F_o)$) and $wR_2(F^2) = 0.0631$ (all data); max./min. residual electron density: 0.362/−0.246 e Å. CCDC-179204 contains the supplementary crystallographic data for this paper. These data can be obtained free of charge via www.ccdc.cam.ac.uk/conts/retrieving.html (or from the Cambridge Crystallographic Data Centre, 12 Union Road, Cambridge CB2 1EZ, UK; fax: (+44) 1223-336-033; or deposit@ccdc.cam.uk).

Acknowledgements

This work was supported by COST (Action 11: "Supramolecular Chemistry"), CNR, MIUR, the EC TMR Research Newtork Programme (contract no. ERBFMRX-CT-98–0226: "Nanometer Size Metal Complexes"), the Nederland Organization for the Advancement of Pure Research (CW-NWO), and by an SNF grant (Denmark) to J.B. C.J.K. also thanks the National Research School Combination Catalysis (NRSC-C), and F.L. thanks the European Community Marie Curie fellowships programme (contract no. HPMF-CT-2000–00622).

  0947-6539/02/0819-4468 $ 20.00+.50/0 *Chem. Eur. J.* **2002**, *8*, No. 19

[1] a) P. Suppan, *Chemistry and Light*, The Royal Society of Chemistry, London, **1994**; b) V. Balzani, *New Scientist* **1994**, *No. 1951*, p. 30; c) J. M. Durrant, *Chem. Ind.* **1998**, October 19, 838; d) M. Freemantle, *Chem. Eng. News* **1998**, October 26; e) M. A. Fox, *Acc. Chem. Res.* **1999**, *32*, 201; f) V. Balzani, S. Serroni, *Science Spectra* **2000**, *22*, 28; g) L. Sun, L. Hammarström, B. Åkermark, S. Styring, *Chem. Soc. Rev.* **2001**, *30*, 36; h) D. Gust, T. A. Moore, A. L. Moore, *Acc. Chem. Res.* **2001**, *34*, 34.

[2] a) S. Campagna, S. Serroni, F. Puntoriero, C. Di Pietro, V. Ricevuto in *Electron Transfer in Chemistry*, *Vol. 5* (Ed.: V. Balzani), Wiley-VCH, **2001**, p. 186, and refs. therein.

[3] a) T. J. Meyer, *Acc. Chem. Res.* **1989**, *22*, 163; b) M. R. Wasielewski, *Chem. Rev.* **1992**, *92*, 432; c) M. N. Paddon-Row, *Acc. Chem. Res.* **1994**, *27*, 18; d) C. A. Bignozzi, J. R. Schoonover, F. Scandola, *Progr. Inorg. Chem.* **1997**, 44, 1. e) L. De Cola, P. Belser, *Coord. Chem. Rev.* **1998**, *177*, 301; f) M.-J. Blanco, M. C. Jiménez, J.-C. Chambron, V. Heitz, M. Linke, J.-P. Sauvage, *Chem. Soc. Rev.* **1999**, *28*, 293.

[4] Probably the first example of composite light-harvesting antenna/charge-separation (supra)molecular system: D. Kuciauskas, P. A. Liddell, S. Lin, T. E. Johnson, S. J. Weghorn, J. S. Lindsey, A. L. Moore, T. A. Moore, D. Gust, *J. Am. Chem. Soc.* **1999**, *121*, 8604. During the preparation of this paper, another article on this subject appeared: A. Wakano, A. Osuka, T. Yamazaki, Y. Nishimura, S. Akimoto, I. Yamuzaki, A. Itaya, N. Murakami, H. Miyasaka, *Chem. Eur. J.* **2001**, *7*, 3134. Antenna systems connected to solid-state charge-separation devices: H. Imahori, H. Norieda, H. Yamada, Y. Nishimura, I. Yamazaki, Y. Sakata, S. Fukuzumi, *J. Am. Chem. Soc.* **2001**, *123*, 100, and references therein.

[5] a) G. Denti, S. Campagna, L. Sabatino, S. Serroni, M. Ciano, V. Balzani, *Inorg. Chem.* **1990**, *29*, 4750; b) V. Balzani, S. Campagna, G. Denti, A. Juris, S. Serroni, M. Venturi, *Acc. Chem. Res.* **1998**, *31*, 26; c) F. Puntoriero, S. Serroni, A. Licciardello, M. Venturi, A. Juris, V. Ricevuto, S. Campagna, *J. Chem. Soc. Dalton Trans.* **2001**, 1035.

[6] a) M. Bryce, *Chem. Soc. Rev.* **1991**, *20*, 355; b) M. B. Nielsen, C. Lomholt, J. Becher, *Chem. Soc. Rev.* **2000**, *29*, 153; c) J. O. Jeppesen, J. Perkins, J. Becher, J. F. Stoddart, *Angew. Chem.* **2001**, *113*, 1256; *Angew. Chem. Int. Ed.* **2001**, *40*, 1216.

[7] a) N. Svenstrup, K. M. Rasmussen, T. K. Hansen, J. Becher, *Synthesis*, **1994**, 809; b) R. R. Ashton, V. Balzani, A. Credi, O. Kocian, D. Pasini, L. Prodi, N. Spencer, J. F. Stoddart, M. S. Tolley, M. Venturi, A. J. P. White, D. J. Williams, *Chem. Eur. J.* **1998**, *4*, 590.

[8] A. Juris, V. Balzani, F. Barigelletti, S. Campagna, P. Belser, A. von Zelewsky, *Coord. Chem. Rev.* **1988**, *84*, 85.

[9] In principle, a more suitable reference for the trinuclear metal complex would be $[\{(bpy)_2Ru(\mu\text{-}2,3\text{-}dpp)\}_2Ru(4,4'\text{-}Mebpy)]^{6+}$, which has never been prepared. However, the redox and photophysical differences between this compound and $[\{(bpy)_2Ru(\mu\text{-}2,3\text{-}dpp)\}_2Ru(bpy)]^{6+}$, taken as a model for **9** and **10**, should be small.

[10] a) *Photoinduced Electron Transfer* (Eds.: M. A. Fox, M. Chanon), Elsevier, New York, **1988**; b) F. Scandola, M. T. Indelli, C. Chiorboli, C. A. Bignozzi, *Top. Curr. Chem.* **1990**, *158*, 73.

[11] Rate constants for electron-transfer quenching are calculated by the equation $k_q = (1/\tau - 1/\tau_0)$, where τ and τ_0 are the excited-state lifetimes of the compound containing the quencher subunit and of the model compound, respectively, obtained from transient absorption and/or luminescence decays.

[12] P. R. Ashton, R. Ballardini, V. Balzani, I. Baxter, A. Credi, M. C. T. Fyfe, M. T. Gandolfi, M. Gómez-López, M.-V. Martínez-Díaz, A. Piersanti, N. Spencer, J. F. Stoddart, M. Venturi, A. J. P. White, D. J. Williams, *J. Am. Chem. Soc.* **1998**, *120*, 11932.

[13] The transient absorption decay of **7** also exhibits a shorter lived, minor component ($\tau = 30$ ps). The origin of this minor component is not discussed here.

[14] P. Chen, T. J. Meyer, *Chem. Rev.* **1998**, *98*, 1439.

[15] H. Berglund Baudin, J. Davidsson, S. Serroni, A. Juris, V. Balzani, S. Campagna, L. Hammarström, *J. Phys. Chem. A*, **2002**, *106*, 4312.

[16] F. Puntoriero, S. Serroni, S. Campagna, J. Andersson, V. Sundström, unpublished results.

[17] V. Balzani, F. Scandola, *Supramolecular Photochemistry*, Ellis-Horwood, Chichester, **1991**, Chapter 5.

[18] One of the referees pointed out that, since the energy transfer in the antenna is ultrafast, up-hill hopping in the reverse direction could occur on a timescale similar to that of the observed quenching. That is, charge separation does not have to be remote, but could occur via transient, reversible hopping to the higher energy chromophore attached to the TTF donor. Similarly, recombination could occur via transient hole hopping. This of course would affect the discussion on forward/backward rates. We agree with the referee that this hypothesis cannot be excluded, but in the absence of clear-cut evidence we prefer to maintain our discussion as presented in the main text. In any case, this mechanistic issue does not alter our conclusions.

[19] Multicomponent metal-based species in which the light absorbed by some component is transferred to a different subunit where it is used to drive a chemical reaction have been reported. See, for example: S. M. Molnar, G. Nallas, J. S. Bridgewater, K. J. Brewer, *J. Am. Chem. Soc.* **1994**, *116*, 5206. However, in the reported systems there was no electron-donor/acceptor group acting as a charge-separation unit.

[20] The use of *trans*-bpy-TTF_1 instead of *cis*-bpy-TTF_1 under the same reaction conditions led to the same final products. The *trans* isomer isomerizes to the *cis* isomer under the conditions used for the preparation of the metal complexes.

[21] SMART: Area Detector Control Software, version 5.054. Bruker AXS Inc., Madison, Wisconsin, USA, **1998**.

[22] SAINT: Area Detector Integration Software, version 6.02a, Bruker AXS Inc., Madison, Wisconsin, USA, **2000**.

[23] G. M. Sheldrick, SADABS, Program for Empirical Correction of Area Detector Data, version 2.01, University of Göttingen, Germany, **2000**.

[24] SHELXTL: Structure Determination Programs, Version 6.12. Bruker AXS Inc., Madison, Wisconsin, USA, **2001**.

[25] A. L. Spek, *Acta Crystallogr. Sect. A* **1990**, *46*, C-34.

Received: February 22, 2002 [F3893]

  0947-6539/02/0819-4469 $ 20.00+.50/0